

# Synchronization of Coupled Kuramoto Oscillators under Resource Constraints

Keith A. Wiley,<sup>1</sup> Peter J. Mucha,<sup>2</sup> and Danielle S. Bassett<sup>3,4</sup>

<sup>1</sup>*Department of Physics & Astronomy, University of Pennsylvania, Philadelphia, PA 19104 USA*

<sup>2</sup>*Departments of Mathematics and Applied Physical Sciences,  
University of North Carolina, Chapel Hill, NC 27599 USA*

<sup>3</sup>*Departments of Physics & Astronomy, Bioengineering, Electrical & Systems Engineering,  
University of Pennsylvania, Philadelphia, PA 19104 USA*

<sup>4</sup>*Santa Fe Institute, Santa Fe, NM 87501 USA*

A fundamental understanding of synchronized behavior in multi-agent systems can be acquired by studying analytically tractable Kuramoto models. However, such models typically diverge from many real systems whose dynamics evolve under non-negligible resource constraints. Here we construct a system of coupled Kuramoto oscillators that consume or produce resources as a function of their oscillation frequency. At high coupling, we observe strongly synchronized dynamics, whereas at low coupling we observe independent oscillator dynamics, as expected from standard Kuramoto models. For intermediate coupling, which typically induces a partially synchronized state, we empirically observe that (and theoretically explain why) the system can exist in either (i) a state in which the order parameter oscillates in time, or (ii) a state in which multiple synchronization states are simultaneously stable. Whether (i) or (ii) occurs depends upon whether the oscillators consume or produce resources, respectively. Relevant for systems as varied as coupled neurons and social groups, our study lays important groundwork for future efforts to develop quantitative predictions of synchronized dynamics for systems embedded in environments marked by sparse resources.

Since their development in 1975 [1], coupled Kuramoto oscillators have been used to model a variety of physical systems [2–5] and understand associated behaviors [6–11]. These applications typically require alterations to the canonical model, including the addition of time-delayed coupling or inertia. However, there is one pervasive discrepancy between the Kuramoto model and real systems that remains relatively unstudied: non-negligible constraints on system resources.

Consequent to thermodynamics, no system can sustain oscillations indefinitely without a supply of some resource. Further, the transition from persistent oscillation to the stationary state is typically not discontinuous as a function of resource supply; it is instead gradual. A mechanical watch, for example, will not suddenly stop ticking as the spring loses its stored potential energy, but will gradually lose seconds over time until the spring has fully unwound. While the dependence on resources may be fairly unimportant during periods of adequate supply, that dependence becomes critical to system behavior when resources become scarce. For example, oxygen deprivation during concussion can perturb the activity of coupled neurons in the human brain, and a scarcity of natural resources can alter predator-prey population cycles in ecology.

We propose a simple model accounting for resource constraints in a system of Kuramoto oscillators. Oscillators are assumed to have resource-dependent internal velocities, to consume resources as a function of their net velocities, and to acquire resources from baths of the resource whose levels are unique to each oscillator. That is, oscillator  $i$  is associated with a resource level,  $R_i$ , which modifies its internal velocity,  $\omega_i(R_i)$ , and is connected to its own thermodynamic resource bath level,  $B_i$ . A sub-

script is included on the function  $\omega_i(\cdot)$  because the functional dependence between oscillation rate and resource level may itself differ among oscillators. Unlike [12], the rate of change of the resource level here is a function of the net velocity and the difference between the current resource level and its bath. Thus, in the most general form, the phases,  $\phi_i$ , and resource levels,  $R_i$ , of our system obey

$$\dot{\phi}_i = \omega_i(R_i) + \frac{K}{N} \sum_j A_{ij} \sin(\phi_j - \phi_i), \quad (1)$$

$$\text{and } \dot{R}_i = f_i(B_i - R_i, \dot{\phi}_i), \quad (2)$$

for  $N$  oscillators coupled with strength  $K$  according to adjacency matrix elements  $A_{ij}$ .

We simplify this general model by assuming linear relationships for  $\omega_i(R_i) = \nu_i + \mu_i R_i$  and  $f_i(B_i - R_i, \dot{\phi}_i) = \alpha_i + D_i(B_i - R_i) + \beta_i \dot{\phi}_i$ . We also assume oscillators are identical in their functional dependencies (i.e.  $\omega_i(x) = \omega_j(x)$  and  $f_i(x, y) = f_j(x, y)$ ), and we thus drop associated  $i$  indices from the expansion coefficients. To eliminate one additional parameter, we redefine  $\dot{\phi}_i$  to  $\dot{\phi}_i - \nu$ . Thus  $\beta_i \dot{\phi}_i$  becomes  $\beta \dot{\phi}_i - \beta \nu$ , and we absorb this second term into our definition of  $\alpha$ . Our final system is

$$\dot{\phi}_i = \mu R_i + \frac{K}{N} \sum_j A_{ij} \sin(\phi_j - \phi_i), \quad (3)$$

$$\text{and } \dot{R}_i = \alpha + D(B_i - R_i) + \beta \dot{\phi}_i. \quad (4)$$

In words,  $\mu$  defines the sensitivity of internal velocity to resource level,  $\alpha$  defines the intrinsic production (if positive) or consumption (if negative) of resource by an oscillator,  $D$  defines the diffusion rate of the resource between bath and oscillator, and  $\beta$  defines the amount of

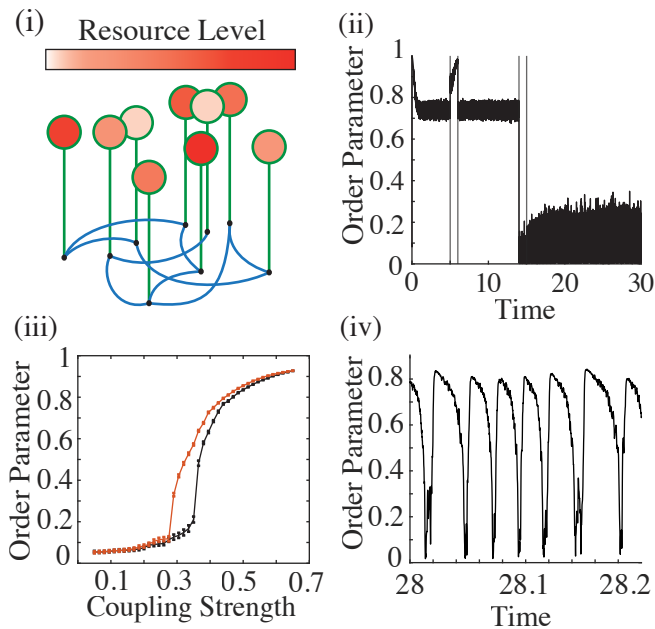


FIG. 1. **Overview of System Behavior.** (i) Schematic of system configuration of oscillators (black points), resource baths (red circles), diffusive connections (green lines), and phase-coupled interactions (blue lines). (ii) Time series of the order parameter in the bistable case. During time 5–6, a perturbation forces the system to synchronize. During time 15–16, a perturbation forces the system to desynchronize. (iii) The temporal mean and standard deviation of the order parameter as a function of the coupling strength, shown both for increasing (black) and then decreasing (red) the coupling strength. We observe swift synchronization when increasing the coupling strength, and bistability is evidenced by the different synchronization levels observed for the same value of the coupling strength. (iv) A sample time series of the oscillating order parameter regime.

resource consumed (if negative) or produced (if positive) per oscillation.

To probe the behavior of this model, we begin by studying a system of 400 oscillators with normally distributed  $B_i$ . Oscillators are coupled on an Erdős-Rényi network with edge probability 0.2, which is large enough to ensure mean field theory can provide a reasonable approximation of the system’s behavior. For analytic simplicity, model parameters are chosen so that the phase timescale is much faster than the resource timescale. Varying  $K$  and  $\beta$ , we evaluate synchronization using order parameter  $r$  defined by  $re^{i\psi} = \frac{1}{N} \sum_j e^{i\phi_j}$  (Fig. 1). In this sample instantiation, we observe four primary behaviors: (i) a fixed point at asynchrony for small  $K$ , (ii) a fixed point at synchrony for large  $K$ , (iii) an oscillating order parameter if  $K$  is intermediate and  $\beta < 0$ , and (iv) bistability if  $K$  is intermediate and  $\beta > 0$ . No other significantly different behaviors were observed for other parameter choices, although some may exist given the size of the parameter space.

We first consider the possible behaviors of a single oscillator interacting with a supposed synchronized group,

and then we turn to group-level dynamics. An oscillator can be considered a two-state system (Fig. 2.i). In the first state,  $S1$ , the oscillator turns with a net velocity equal to the average velocity of the group ( $\dot{\phi}_i = \Omega$ ); in the second state,  $S2$ , the oscillator turns with a net velocity equal, on average, to its internal velocity ( $\dot{\phi}_i = \omega_i = \mu R_i$ ). Because the equilibrium resource level is defined in part by the net velocity, and because the internal velocity is defined by resource level, each of the states  $S1$  and  $S2$  will have corresponding equilibrium internal velocities  $\omega_i(S1)$  and  $\omega_i(S2)$  that the oscillator will approach over time. Further, an effective coupling strength is defined in mean field theory, given the size of the current synchronized group and the coupling strength. This effective coupling defines an envelope in frequency space whose boundaries are  $\Omega \pm Kr/N$  (Fig. 2.ii). Refer to the  $SI$  for a derivation of this envelope. If an oscillator’s internal velocity  $\omega_i$  places it within the envelope, it will be captured by (i.e. synchronize with) the group, and if  $\omega_i$  places it outside of the envelope, it will remain free (i.e. unsynchronized).

The possible dynamics of a single oscillator can thus be separated into 4 types. A Type 1 (‘Stably Free’) oscillator is one for which both  $\omega_i(S1)$  and  $\omega_i(S2)$  are outside of the envelope, so that the oscillator will always eventually transition to state  $S2$ . A Type 2 (‘Stably Captured’) oscillator is one for which both  $\omega_i(S1)$  and  $\omega_i(S2)$  are inside of the envelope. A Type 3 (‘Transitory’) oscillator has  $\omega_i(S1)$  outside the envelope and  $\omega_i(S2)$  inside the envelope and will continually alternate between capture and escape. A Type 4 (‘Bistable’) oscillator has  $\omega_i(S1)$  inside the envelope and  $\omega_i(S2)$  outside the envelope, so both states  $S1$  and  $S2$  will be stable. Note that these four behaviors do not depend on any of the simplifications made to the general model. Further, note that the four different group behaviors are not in one-to-one correspondence with these four single-oscillator behaviors, as will be elaborated below. Finally, in the context of our simplified model, we can show that if  $\beta$  and  $\mu$  have the same sign, then Type 4 (‘Bistable’) oscillators may exist; whereas if  $\beta$  and  $\mu$  have opposite signs, then Type 3 (‘Transitory’) oscillators may exist (see the SI). Thus, since the choices of  $\beta$  and  $\mu$  are system-wide, only one of Type 3 and Type 4 oscillators may exist.

Having defined the behavior of a single oscillator interacting with a dominant synchronized group, we now turn to the question of group behaviors. Such group behaviors can be understood by considering the effects of dynamics on the available resources. A Type 1 (‘Stably Free’) oscillator’s resource level will equilibrate to that characteristic of desynchronization. A Type 2 (‘Stably Captured’) oscillator’s resource level will equilibrate to that characteristic of synchronization. The resource level of a Type 3 (‘Transitory’) oscillator will oscillate back and forth between levels characteristic of synchronization and desynchronization, and as a result will pile up at the boundaries of the synchronization envelope. By symmetry of the envelope, Type 3 oscillators will pile up both

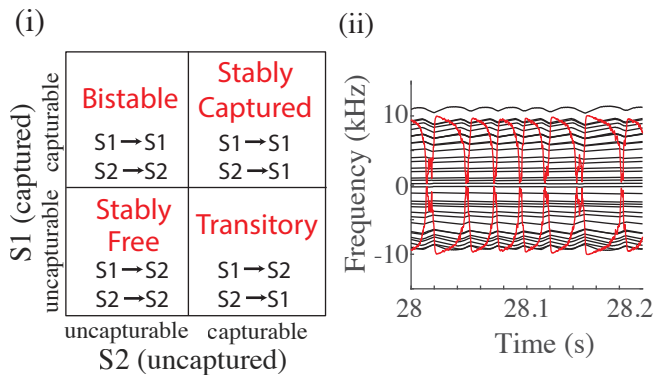


FIG. 2. **Available State Transitions.** (i) The four possible states of a given oscillator subject to its present effective coupling strength to the rest of the group. (ii) The envelope in which an oscillator can be captured. Here the effective coupling strength ( $Kr/N$ ; red) is overlaid on the distance of each oscillator’s internal velocity from the group velocity, defined as the average of all internal velocities, and scaled by the degree of that oscillator (black).

above and below the mean resource level, and so both the resource distribution and in turn the internal velocity distribution of Type 3 oscillators will become bimodal over time. For Type 4 oscillators, their distribution will be smooth over resource levels, but will depend on the history of the system.

In order to understand the transitions observed in the order parameter, we consider graphical solutions to a mean field Kuramoto system

$$r = \frac{Kr \langle d \rangle}{N} \int_{-\frac{\pi}{2}}^{\frac{\pi}{2}} d\omega g\left(\frac{Kr \langle d \rangle}{N} \sin \omega\right) \cos^2(\omega), \quad (5)$$

where  $\omega$  is the internal velocity,  $\langle d \rangle$  is the average degree, and  $g(x)$  is related to the probability distribution of internal velocities (see Fig. 3 and the SI for derivation). Solutions at a chosen moment provide order parameters that would be stable in the mean field description of a system of Kuramoto oscillators with natural velocities equal to their value at that same chosen moment. In fact, the natural velocities of the oscillators drift over time, but because the phase timescale is much faster than the resource timescale, the system will equilibrate its phase behavior before resource levels change appreciably, and therefore this equation is sufficient.

To gain further intuition, suppose the system is presently in some synchronization state with order parameter  $r^*$  (Fig. 3). The right side of Eq. 5 then gives the equilibrium order parameter of the system if each oscillator interacted with a single mean field oscillator with coupling strength  $Kr^* \langle d \rangle / N$ . Call this order parameter  $r'$ . If  $r' > r^*$ , we expect order in the system to increase; if  $r' < r^*$ , we expect order to decrease. This simple argument captures the stability properties of many Kuramoto systems. For example, it correctly predicts the stability properties of Gaussian, unimodal, and (weakly) bimodal natural frequency distributions (Fig. 3.i).

Now we have all of the tools to understand the time evolution of the oscillatory order that we observed. Suppose we let a system of oscillators run for some period of time, and at a given moment we find the order parameter to be large. For a given present value of the order parameter, some of our oscillators will be Type 1, some Type 2, and some Type 3. The resource levels of Type 1 and Type 2 oscillators will be spread over some range, but the Type 3 oscillators will drive a bimodal resource distribution, generating bistability in the system (Figure 3.ii, top left). For the system to be in a high order state, it must be that many of the Type 3 oscillators are currently synchronized inside of the envelope. Thus, these oscillators will gradually move outward toward the boundary of the synchronization envelope. At the group level, this process has the effect of pushing the upper bump of the blue curve downward. Eventually, a saddle-node bifurcation occurs and the high-order solution vanishes. Thus, the system must transition to the low-order state, causing the synchronization envelope to shrink dramatically. Consequently, all of the Type 3 oscillators, no matter their present state, will desynchronize (Fig. 3.ii, top right).

As a result of now being outside of the envelope, the resource levels of all Type 3 oscillators will now move quickly toward the mean level, clustering closely together in resource space. The high-order solution will almost immediately reappear as the Type 3 oscillators begin to cluster together (Fig. 3.ii, bottom left, reflecting a moment of stable disorder). However, since the low-order solution is stable, the system will persist in the low-order state until the Type 3 oscillators cluster sufficiently that the low-order state becomes unstable. For reasons discussed in the SI, in a finite-sized system, this will be the moment when the “energy barrier” between the low- and high-order states becomes sufficiently small that the system can randomly transition to the high-order state (Fig. 3.ii, bottom right). In an infinite-sized system, the details of this transition are unknown to the present authors. Once such a transition occurs, we find the system again in a state of high order (Fig. 3.ii, top left), and the cycle repeats.

Now that we understand group behaviors for Type 3 oscillators, we turn to Type 4 oscillators. Recall that an oscillator’s classification depends upon the present effective coupling strength. With zero coupling, the system will be made up entirely of Type 1 oscillators. If we then increase the coupling, some of the oscillators will become Type 4 oscillators, which being previously unsynchronized, remain unsynchronized. This point in the system’s dynamics is precisely a subcritical bifurcation, since if we moved all of the Type 4 oscillators inside of the envelope, they would remain there and form a stable synchronized group. As we continue to increase the coupling strength, eventually some of the Type 4 oscillators will become Type 2 oscillators, and a small synchronized group of Type 2 oscillators will appear. Upon changing from Type 4 to Type 2 oscillators, the internal veloci-

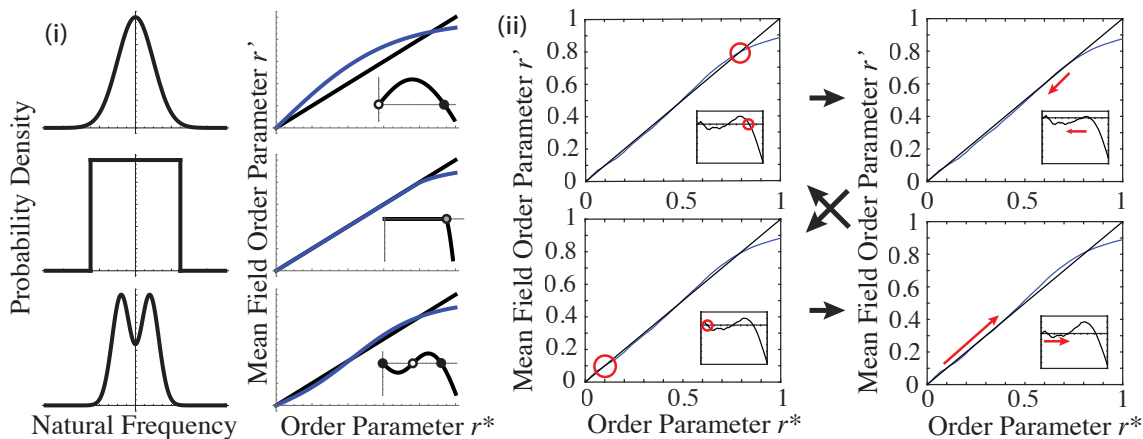


FIG. 3. **Evolving Order of Type 3 ‘Transitory’ oscillators.** (i) *Left* Example natural frequency distributions. *Right* Graphical solutions to the mean field system for the adjacent natural frequency distributions. The present order parameter of the system is marked by  $r^*$ . The mean-field order parameter with effective coupling strength  $K_{\text{eff}} = Kr^*(d)/N$  is marked by  $r'$ . The blue curve gives  $r'$  as a function of  $r^*$ , while the black curve is the line  $r' = r^*$ . Points where the blue and black curves intersect are predicted steady-states of the order parameter for the system. The inset figures give the difference between the blue and black curves. Open circles in the inset figures represent unstable equilibria; black circles represent stable equilibria; and the grey circle represents metastable equilibrium. The top two subfigures give the solution for a Gaussian distribution of natural frequencies, the middle two for a uniform distribution, and the bottom two for a bimodal internal frequency distribution. (ii) The graphical solution at four different moments of the time evolution of the oscillating order parameter system. Red circles indicate the present order parameter of the system. Red arrows indicate that the system’s order parameter is quickly changing in that direction. Black arrows indicate the temporal sequence of the four states. States were chosen such that the top left was a moment of stable synchronization, top right was a moment of desynchronization, bottom left was a moment of stable disorder, and bottom right was a moment of resynchronization.

ties will transition from  $\omega_i(S1)$  to  $\omega_i(S2)$ , causing the order parameter of the system to continually increase, even without changes in the coupling strength. The additional growth will capture more oscillators, initiating a cascade of synchronization. Thus, the system will experience a transition up to the synchronized phase which is first-order in the coupling strength, commonly referred to as explosive synchronization [13].

If we then turn the coupling strength down slowly, the Type 2 oscillators will again become Type 4 oscillators as the synchronization envelope narrows, but high order will persist. Eventually, some of the Type 4 oscillators will become Type 1 oscillators, and so move outside of the envelope of synchronization. However, unlike the case of synchronization, all unsynchronized oscillators are equivalent in their effect on the order parameter. Thus, the transition from  $\omega_i(S2)$  to  $\omega_i(S1)$  will not cause additional change in the order parameter. Consequently, the transition back to disorder will be continuous in the coupling strength; in other words, a second order phase transition.

The behavior of this Kuramoto model can clarify dynamics observed in many physical and biological systems existing under resource constraints. For example, transient oscillatory synchrony has been observed to be important for efficient routing of information [14] in neural systems. Consider also alcohol consumption in a group of acquaintances; each individual will have a preferred frequency of consumption, but their actual frequency will be modulated by interaction with the group. Each in-

dividual also accrues the resource of craving at a different rate based on environmental stimuli such as advertisements, experiences, and inter-personal communication [15]. Consumption can either increase or decrease craving; for some, satiating the urge, while for others, strengthening it. Oscillations in this context are reminiscent of binge drinking behaviors, in which an individual is usually satisfied to drink at a group frequency, but eventually their craving grows until they break off and drink at a higher-than-average frequency for a brief period, after which they settle back into the group frequency. Future studies could exercise the model to study such resource-constrained biological, physical, social, and technological systems, and to better understand their associated behaviors.

Many open questions remain in this system. The social context above motivates consideration of mixed populations of  $\beta > 0$  and  $\beta < 0$  oscillators. In addition, the nature of the connection topology is an important modulator of observed dynamics in standard Kuramoto systems, and we expect the same to be true here. One particularly interesting topological modification would be to connect the baths in the resource level, encoding a multilayer network structure [16] that allows individual oscillators to interact with a shared resource environment. Although resource-constrained Kuramoto systems have been little-considered up to this point, we hope that the interesting behavior observed in just the simplest version of this model motivates further work moving forward.

**Acknowledgements.** We thank Lia Papadopoulos, Zhixin Lu, and Erfan Nozari for providing valuable feedback. This work was primarily supported by the Army Research Office (W911NF-18-1-0244), the Paul G. Allen Foundation, and the NSF through the University of Pennsylvania Materials Research Science and Engineering Center (MRSEC) DMR-1720530. PJM also acknowledges support from the James S. McDonnell Foundation 21st Century Science Initiative - Complex Systems

Scholar Award grant #220020315 and the NSF (ECCS-161076). The content is solely the responsibility of the authors and should not be interpreted as representing the official views or policies, either expressed or implied, of any of the funding agencies. The U.S Government is authorized to reproduce and distribute reprints for Government purposes notwithstanding any copyright notation herein.

- 
- [1] Y. Kuramoto, in *International symposium on mathematical problems in theoretical physics* (Springer, Berlin, Heidelberg, 1975) pp. 420–422.
  - [2] B. Ermentrout, *Journal of Mathematical Biology* **29**, 571 (1991).
  - [3] H. Sompolinsky, D. Golomb, and D. Kleinfeld, *Proceedings of the National Academy of Sciences of the United States of America* **87**, 7200 (1990).
  - [4] G. Kozyreff, A. G. Vladimirov, and P. Mandel, *Physical Review E* **64**, 016613 (2001).
  - [5] G. Filatrella, A. H. Nielsen, and N. F. Pedersen, *The European Physical Journal B* **61**, 485 (2008).
  - [6] D. A. Wiley, S. H. Strogatz, and M. Girvan, *Chaos: An Interdisciplinary Journal of Nonlinear Science* **16**, 015103 (2006).
  - [7] J. Gómez-Gardeñes, S. Gómez, A. Arenas, and Y. Moreno, *Physical Review Letters* **106**, 128701 (2011).
  - [8] D. Pazó and E. Montbrió, *Physical Review E* **80**, 046215 (2009).
  - [9] H. Hong and S. H. Strogatz, *Physical Review E* **84**, 046202 (2011).
  - [10] J. A. Acebrón, L. L. Bonilla, C. J. Pérez Vicente, F. Ritort, and R. Spigler, *Reviews of Modern Physics* **77**, 137 (2005).
  - [11] S. Olmi, *Chaos: An Interdisciplinary Journal of Nonlinear Science* **25**, 123125 (2015).
  - [12] V. Nicosia, S. Skardal, A. Arenas, and V. Latora, (2017), arXiv:arXiv:1405.5855v7.
  - [13] R. M. D’Souza, J. Gomez-Gardenes, J. Nagler, and A. Arenas, *Advances in Physics* **68** (2019).
  - [14] A. Palmigiano, T. Geisel, F. Wolf, and D. Battaglia, *Nature Neuroscience* **20**, 1014 (2017).
  - [15] D. Seo and R. Sinha, *Handbook of Clinical Neurology* **125**, 355 (2014).
  - [16] G. Bianconi, *Multilayer Networks: Structure and Function* (Oxford University Press, 2018).